SCIENCE CHINA
Technological Sciences

Concept of the Solar Ring mission: Preliminary design and mission profile

YaMin WANG, Xin CHEN, PengCheng WANG, ChengBo QIU, YuMing WANG and YongHe ZHANG

Citation: SCIENCE CHINA Technological Sciences; doi: 10.1007/s11431-020-1612-y

View online: http://engine.scichina.com/doi/10.1007/s11431-020-1612-y

Published by the Science China Press

SCIENCE CHINA
Technological Sciences

•Article•

https://doi.org/10.1007/s11431-020-1612-y

Concept of the Solar Ring mission: Preliminary design and mission profile

WANG YaMin[1,2,3], CHEN Xin[1,2,3], WANG PengCheng[1,2,3], QIU ChengBo[1,2,3], WANG YuMing[4,5] & ZHANG YongHe[1,2,3*]

[1] *Innovation Academy for Microsatellites, Chinese Academy of Sciences (CAS), Shanghai 201203, China;*
[2] *Key Lab of Microsatellite, Chinese Academy of Sciences, Shanghai 201203, China;*
[3] *Shanghai Engineering Center for Microsatellites, Shanghai 201203, China;*
[4] *CAS Key Laboratory of Geospace Environment, School of Earth and Space Sciences, University of Science and Technology of China, Hefei 230026, China;*
[5] *CAS Center for Excellence in Comparative Planetology, University of Science and Technology of China, Hefei 230026, China*

Received February 25, 2020; accepted April 24, 2024; published online May 19, 2020

The Solar Ring mission, a concept to monitor the Sun and inner heliosphere from multiple perspectives, has been funded for pre-phase study by the Strategic Priority Program of Chinese Academy of Sciences in space sciences. The Solar Ring is comprised of 6 spacecraft, grouped in three pairs, moving around the Sun in an elliptical orbit in the ecliptic plane. The mission costs, including launch fee, deep-space maneuvers, and deployment time of the ring, are highly relevant to the working orbit, deep-space transfer, and phase angle within a group. The preliminary mission profile is analyzed and designed in this paper. The launch way, two spacecraft with one rocket, is adopted. The deployment time, phasing maneuvers, and C_3 of launch energy are evaluated for the elliptical orbits with the perihelion between 0.7 and 0.9 AU using the rockets of Long March (LM) 3A and 3B. Numerical simulations show two candidate trajectories: fast deployment within 4 years by LM-3B, medium deployment more than 6 years by cheaper rocket of LM-3A. In order to obtain both fast deployment and low launch cost, another orbit profile is proposed by shortening the phase angle within a group. The suggested working orbits and the corresponding costs of launch, deployment time, and phasing maneuvers will strongly support the science objectives.

solar and heliospheric observations, deep-space transfer, orbit optimization

Citation: Wang Y M, Chen X, Wang P C, et al. Concept of the Solar Ring mission: Preliminary design and mission profile. Sci China Tech Sci, 2020, 63, https://doi.org/10.1007/s11431-020-1612-y

1 Introduction

In the past decades, several solar observatory spacecraft have been launched into the interplanetary space [1], Sun-Earth L1 [2–4] and Earth orbits [5–9]. The mission profile of the observatory is closely related to the science objectives and mission cost. The undergoing mission Solar TErrestrial RElations Observatory (STEREO), launched in 2006, is the first mission to provide stereoscopic measurements of the Sun and the heliosphere [1]. Two nearly identical observatories of STEREO are launched into orbits circling around the Sun in a low-cost launch way, the lunar swing-by, with one observatory moving on an inner Earth orbit called ‘‘ahead’’ and the other moving on an outer Earth orbit called ‘‘behind’’ [1]. Recently, Parker Solar Probe (PSP) flew to as close as 9.5 solar radii from the Sun to sample the solar corona [10]. The extremely low perihelion orbit is constructed by a series of Venus gravity assists. Solar Orbiter, an observatory to observe the Sun from middle-to-high latitude, has been launched to the resonance orbit of Venus on Feb-

*Corresponding author (email: zhangyh@microsate.com)

ruary 10, 2020 for inclination raise with gravity assist of Venus to explore the poles of Sun [9]. The under-development mission Advanced Space-based Solar Observatory (ASO-S), the first Chinese space-based solar observatory mission, is planned to launch in 2021 and move on the 700 km sun-synchronous orbit [11]. Its aims are to observe and to study the origin of the solar magnetic fields, solar flares and coronal mass ejections and the possible causal relationship among them.

The real-time observations of the full solar disk in 360°, especially for the full-disk magnetic field measurements, have not yet achieved. The concept of the Solar Ring mission, funded for the pre-phase study by the Strategic Priority Program of Chinese Academy of Sciences in space sciences in May 2019, proposes to unambiguously measure the photospheric vector magnetic fields, provide 360° maps of the Sun and the inner heliosphere, and resolve solar wind structures at multiple scales and multiple longitudes. The Solar Ring constellation, comprised of 6 spacecraft, is deployed around the Sun in elliptical orbits located on the ecliptic plane [12]. Each spacecraft carries the remote sensing and *in-suit* instruments to address the science objectives: (1) the origin of solar cycle, (2) the origin of solar eruptions, (3) the origin of solar wind structures, and (4) the origin of the severe space weather events [13].

In this paper, several topics related to the working orbit and phasing trajectory are discussed for better understanding of the connection among the perihelion radius r_p of working orbit, phase angle α within each group, total mass of spacecraft, rocket capability, deployment time of constellation, etc. Concretely, the following aspects are touched. (1) Carrying capability of rocket associated with the perihelion of r_p. Rocket capability is crucial since it constrains the spacecraft mass. The rocket capability and the elliptical working orbit are connected by launch energy C_3. Based on the relationship between launch capability and C_3 [14], the curves of launch capability of LM-3A and LM-3B with r_p of [0.7, 0.9] AU are obtained. (2) Phasing maneuvers associated with r_p and phase angle α. "Two spacecraft with one rocket" is a preferential launch way for lowering the rocket cost in this mission. Thus, a group of spacecraft is launched to the same orbit around the Sun simultaneously. Phasing maneuvers executed by spacecraft itself are necessary. By the optimization algorithm, the optimal phasing maneuvers are obtained for each pair of r_p and α. (3) Deployment time of the constellation associated with the r_p. Deployment time dt of the mission includes dt_1 of phasing time for the phasing spacecraft, dt_2 and dt_3 of time intervals for three launches. The phasing time dt_1 associated with the optimal phasing trajectory is calculated by trajectory optimal algorithm. Rate of departure from the Earth of the spacecraft with r_p between 0.7–0.9 AU is calculated to evaluate dt_2. (4) The solution in the r_p-α plane on the constraints of rocket and deployment time. Based on the constraints, fast, medium, and slow deployment profiles, corresponding to different regions in r_p-α plane, are identified. Three feasible trajectories belong to different region are designed and analyzed.

2 Requirements of mission design from science objectives

According to refs. [12,13], 6 spacecraft, moving around the Sun on an ecliptic plane, form a stereo observational network. The 6 spacecraft are grouped in three pairs. In each pair, the two spacecraft are separated by about 30°, and between the pairs, the separation angle is about 120° (or about 90° between the two closest spacecraft). This deployment not only achieves the entire 360° view of the Sun, but also provides different stereoscopic views with the angle of about 30°, 90°, 120° and 150°. By using this configuration, Solar Ring mission will perform high resolution imaging of from photosphere to inner heliosphere and qusi-heliosynchronous *in-situ* sampling of particles and fields. The illustration of stereo observation is shown in Figure 1. Several requirements for mission design are summarized as follows: (1) 6 spacecraft are grouped into three pairs with 120° phase angle β; (2) within each group, two spacecraft are departure with 30° phase angle α; (3) considering the cost of launch and fuel, working orbits for 6 spacecraft are elliptical orbits around the Sun with the perihelion between 0.7 and 0.9 AU and the aphelion of 1 AU; (4) deployment time of the total 6 spacecraft should be quick and less than 4 years.

3 Working orbits constructed by "two spacecraft with one rocket"

3.1 Deployment strategy and algorithm

As suggested in ref. [13], the phase angle α within each

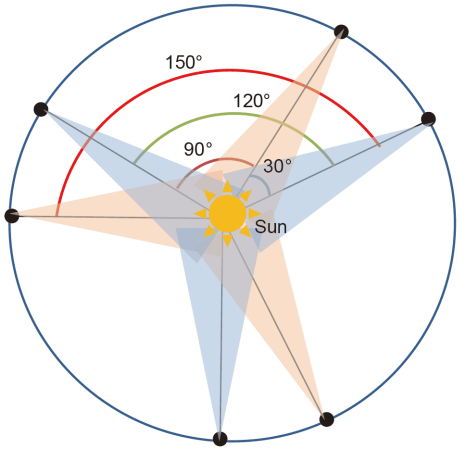

Figure 1 Illustration of stereo observation for the Solar Ring mission.

group is 30°, meaning that one (A_1 spacecraft) of two spacecraft, launched by one rocket, should maneuver to depart from A_2 spacecraft ahead or behind by 30°. Two kinds of relation positions of A_1 and A_2 spacecraft, the "ahead" and "behind", illustrated in Figure 2, require different deployment time and maneuvers. Three groups of spacecraft need three launches. The launch times of the second and the third groups depend on the angular rate of spacecraft departure with respect to the Earth. The launch opportunity appears when the departure angle of spacecraft launched last time away from the Earth reaches 120°.

The phasing trajectory is designed by the way of two-impulse transfer and is shown in Figure 3. After launch, A_1 and A_2 spacecraft fly along the working orbit together for some time t_1. Then, spacecraft A_1 performs the first maneuver ΔV_1 to depart from the working orbit and insert into phasing trajectory. The second maneuver ΔV_2 is executed when the phasing trajectory intersects with the working orbit. The flight time of phasing trajectory is ft. Finally, the A_1 and A_2 spacecraft move in the same orbit and depart with 30° phase angle. Since the orbital period of phasing trajectory is shorter or longer than that of the working orbit, A_1 spacecraft

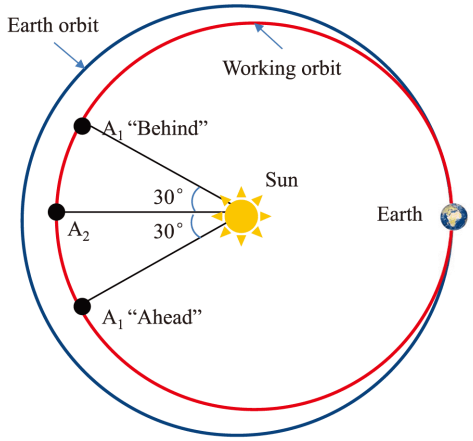

Figure 2 Sketch of "behind" and "Ahead" of A1 spacecraft relative to A2 spacecraft.

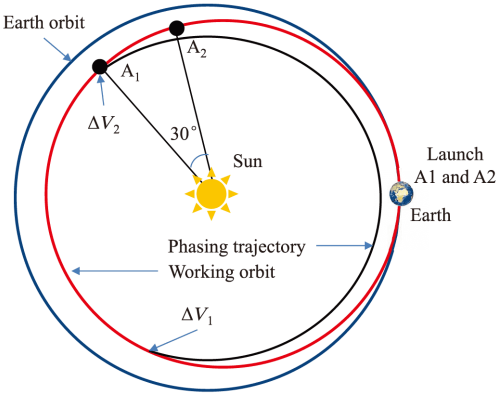

Figure 3 Sketch of two-impulse transfer of phasing trajectory.

can move faster or slower than A_2, which results in the "ahead" or "behind" configuration.

All simulations in this paper use the heliocentric dynamics model which can be found below.

$$\ddot{\mathbf{r}} = \frac{\mu}{\mathbf{r}}, \tag{1}$$

where μ is the gravitational constant of the Sun and $\mathbf{r}$ is the position vector of spacecraft relative to the sun in the inertial frame.

According to the theory of two-point boundary value problem (TPBVP) [15], the phasing trajectory can be calculated by the position $\mathbf{R}_1$ where the first maneuver ΔV_1 occurs, position $\mathbf{R}_2$ of maneuver ΔV_2, and the flight time ft of phasing trajectory. Accurately, both $\mathbf{R}_1$ and $\mathbf{R}_2$ locate on the working orbit. Defining $\mathbf{f}_1$ as the trajectory propagator function [16], $\mathbf{R}_1$ and $\mathbf{R}_2$ can be obtained by

$$\begin{aligned} \mathbf{R}_1 &= \mathbf{f}_1(\mathbf{R}_0, t_1), \\ \mathbf{R}_2 &= \mathbf{f}_1(\mathbf{R}_0, t_1 + ft, \alpha), \end{aligned} \tag{2}$$

where $\mathbf{R}_0$ is the position of A_1 spacecraft/Earth with respect to Sun at the time of launch and α is the phase angle within each group. Then, the phasing trajectory can be solved by

$$[\Delta\mathbf{V}_1, \Delta\mathbf{V}_2] = \mathbf{f}_2(\mathbf{R}_2, \mathbf{R}_1, ft), \tag{3}$$

where $\mathbf{f}_2$ is the algorithm of TPBVP. In conclusion, the phasing trajectory is determined by three variables, ft, $\mathrm{d}t_1$ and α. However, the value of α is desired to be 30° from the view of science. A global optimization algorithm, genetic algorithm (GA) [17], is adopted to get the minimum total $\Delta V = \Delta V_1 + \Delta V_2$ and the corresponding values of variables ft and $\mathrm{d}t_1$.

3.2 Analysis of phasing maneuvers

In the two-dimensional space of phase angle α and the perihelion distance r_p, each point corresponds to an optimal total maneuver ΔV of phasing trajectory which is calculated by the algorithm mentioned above in Sect. 3.1. The total maneuvers for both "ahead" and "behind" deployment are calculated and analyzed with $r_p \in [0.7, 0.9]$ AU and $\alpha \in [15°, 30°]$. It is worth mentioning that phase angle α is no longer a fixed value of 30°, but ranges from 15° to 30°. We want to explore the impact of both phase angle α and perihelion r_p on phasing trajectory.

The results for the phasing trajectory of "ahead" and "behind" deployment are shown by the contour maps in Figure 4(a) and (b), respectively. The contour lines in these figures represent the magnitude of total phasing maneuvers ΔV. The ΔV is positively correlated with phase angle α and is negatively correlated with perihelion radius r_p. In both Figure 4(a) and (b), the total maneuver reaches its maximum value when the perihelion radius is 0.7 AU and phase angle is 30°, and reaches its minimum value when the perihelion radius is 0.9 AU and the phase angle is 15°. Obviously, the

total ΔV of "ahead" deployment is greater than that of "behind" deployment. The minimum and maximum ΔV for "ahead" deployment is about 0.93 and 2.32 km/s, and is about 0.85 and 1.87 km/s for the "behind" deployment, respectively. The total maneuver is highly relative to the fuel consumption and the total mass of spacecraft as well as the launch fee. Thus, the mean of "behind" deployment will be adopted in the trajectory design. Meanwhile, greater perihelion and smaller phase angle α is the better choice from the viewpoint of total maneuver.

3.3 Analysis of deployment time

Deployment time dt of the Solar Ring consists of three parts, the time dt_1 for accomplishment of 30° phase, the time dt_2 of interval between 1st and 2nd launches, and time dt_3 of interval between 2nd and 3rd launches. The phasing time dt_1 is obtained by the optimal design of phasing trajectory. The time dt_1 of phasing trajectory, which is $ft+t_1$, for "ahead" and "behind" deployment are shown in Figure 5(a) and (b) using contour map, respectively.

From this figure, the phasing time dt_1 is positively correlated with r_p for both "ahead" and "behind" deployment. However, dt_1 shows an anti-correlation with phase angle α for the "ahead" case, but the positive correlation with α for the "behind" deployment. It means fast phasing requires small r_p and large α for "ahead" deployment or small r_p and small α for "behind deployment". The minimum and maximum dt_1 for "ahead" deployment is about 395 days/1.08 years and 488 days/1.34 years, and is about 445 days/1.22 years and 533 days/1.46 years for the "behind" deployment, respectively. Obviously, the phasing time dt_1 of "ahead" deployment is less than that of "behind" deployment. Nevertheless, "ahead" deployment requires more phasing maneuver as mentioned above in Sect. 3.2. Meanwhile, in the "ahead" deployment, the optimal phase angle α

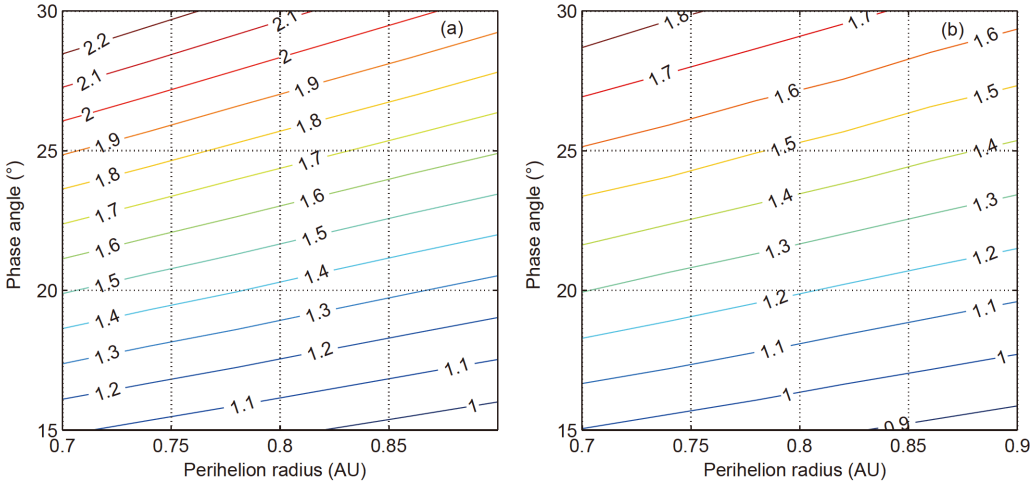

Figure 4 (a) Contour map of the total maneuver for "ahead" spacecraft; (b) contour map of the total maneuver for "behind" spacecraft (the curves in figures are the total maneuver for phasing trajectory, the unit of maneuver is km/s).

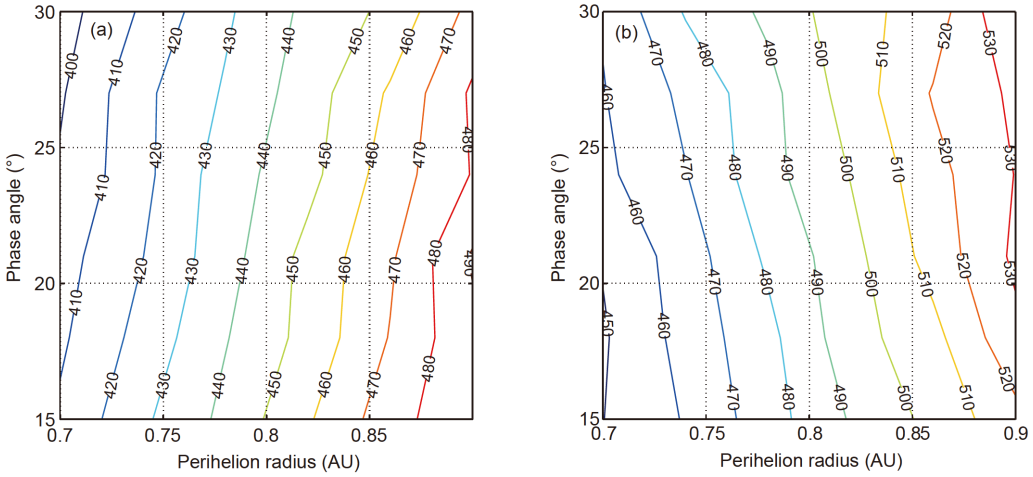

Figure 5 (a) Contour map of the phasing time for "ahead" deployment; (b) contour map of the phasing time for "behind" deployment (the curves in figures are the total flight time for phasing trajectory; the unit of flight time is day).

for maneuver and phasing time are divergent, i.e., α of 30° benefit the fast deployment, conversely, α of 15° benefits the small phasing maneuver.

Moreover, the time interval dt_2 and dt_3 between launches are analyzed. The time interval depends on the angle rate of spacecraft departure from the Earth. The departure angle for several working orbits with perihelion from 0.7 to 0.9 AU are calculated and shown in Figure 6. When the departure angle reaches 120°, the next group of spacecraft can be launched. The simulation result demonstrates that the launch interval is 1.19 years for r_p=0.7 AU, 1.33 years for r_p=0.75 AU, 2.07 years for r_p=0.8 AU, 2.54 years for r_p=0.85 AU, and 4.18 years for r_p=0.9 AU.

The launch interval is positively correlated with r_p. However, the relationship is not linear. In order to identify the fast, medium, and slow phasing deployment, the curve of deployment time dt is calculated, and is shown in Figure 7. We can find four small-slope regions with r_p within 0.7–775 AU, 0.78–0.85 AU, 0.855–0.885 AU, and 0.89–0.9 AU, respectively, which have been marked in this figure. The dt in the first region ranges from 3.6 to 4.3 years that means r_p located between 0.7 and 0.775 AU will result in fast deployment. Then, the deployment time dt is growing rapidly and enters to second region with r_p in 0.78–0.85 AU which is named medium deployment. The medium deployment takes 5.1–6.2 years to finish constellation deployment of the Solar Ring. The rest regions have the dt more than 7 years, and are not considered in this mission.

3.4 Analysis of carrying capabilities of rockets

The carrying capability of rocket for deep-space mission depends on the launch energy C_3. $C_3 = V_\infty^2$. V_∞ is the hyperbolic excess velocity of spacecraft with respect to the Earth on the boundary of Earth's sphere of influence, and can be derived from the perihelion radius and aphelion radius of working orbit by two-body orbit theory. The launch energy C_3 corresponding to the elliptical orbit with 0.7–1 AU perihelion and 1 AU aphelion is calculated and shown in Figure 8 (marked by the green line). The maximum C_3 is 0.77 km^2/s^2 when the perihelion is 0.7 AU. Then, C_3 decreases with increasing perihelion, and approaches to 0 km^2/s^2 when the perihelion reaches 1 AU.

The Chinese LM-3 series rocket can launch the deep-space spacecraft. The carrying capabilities of two kinds of rockets, LM-3A and LM-3B, are calculated and are shown in Figure 8 (dash blue line for LM-3A and solid blue line for LM-3B). The carrying capability is about 1070 kg for LM-3A and 2760 kg for LM-3B when the C_3 is 0.77 km^2/s^2 corresponding to 0.7 AU perihelion. When the C_3 reduces, the launch mass increases until 1450 kg for LM-3A and 3300 kg for LM-3B when the C_3 is 0 km^2/s^2 corresponding to 1 AU perihelion. The carrying capability of LM-3B is more than two times of that of LM-3A.

Obviously, perihelion radius determines the launch C_3 and

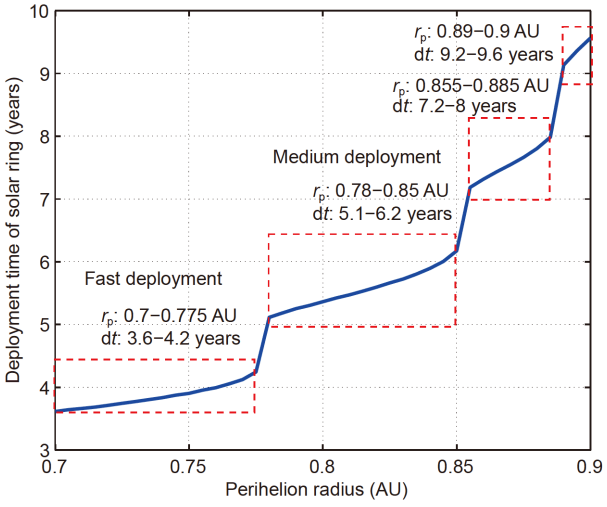

Figure 7 Deployment time with perihelion radius.

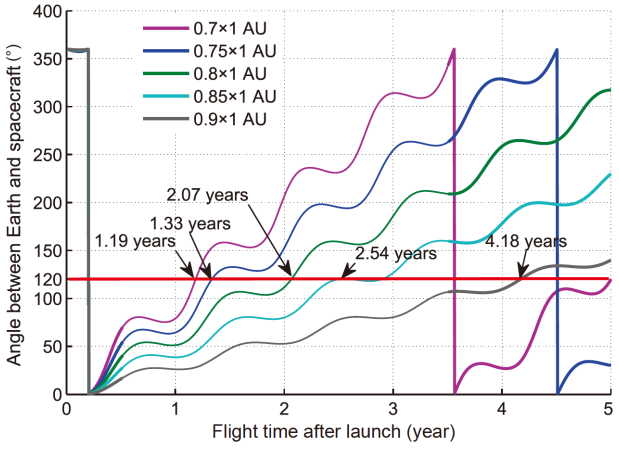

Figure 6 Departure angle from the Earth for working orbit of different perihelion radius.

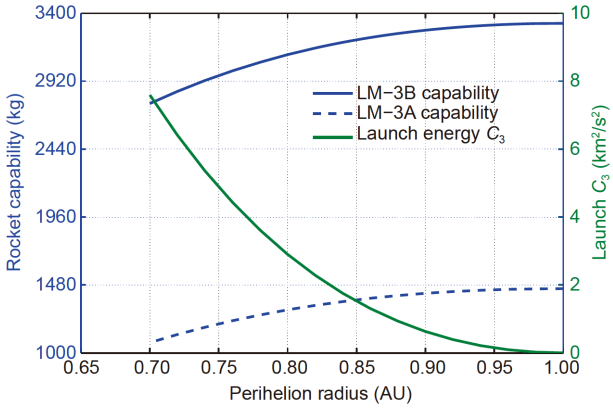

Figure 8 Relationship between carrying capabilities of rockets, launch energy C_3 and perihelion radius of working orbit.

the carrying capability of the rocket. Large perihelion radius allows more carrying capability. The launch mass should be distributed to two spacecraft launched together after calculating the upper limit M_{up} of carrying capability of rocket. First, we need to calculate whether the M_{up} is sufficient for "two spacecraft with one rocket". Noting the dry mass of spacecraft A_2 as M_{dry}, the mass of fuel required for phasing maneuver as M_{fuel}, we have the mass of phasing spacecraft A_1 as $M_{wet}=M_{dry}+M_{fuel}$. Since the mass of a spacecraft bus is about 350 kg, plus the science payloads of which the mass is about 110 kg [13], the dry mass M_{dry} is estimated to be about 460 kg. $M_{wet}+M_{dry}<M_{up}$ is the "two spacecraft with one rocket" requirement for the rocket.

In the following section, the fuel consumption and the deployment time of the Solar Ring associated with the perihelion radius will be discussed to provide the optimal perihelion radius.

3.5 Characterize the solution space

We have found that smaller phasing maneuver requires larger perihelion radius r_p and smaller phase angle α, while faster deployment requires smaller perihelion radius r_p. Meanwhile, both phasing maneuver and deployment time are constrained by the carrying capability of the rocket. The design of phasing trajectory and working orbit of the Solar Ring in the r_p-α two-dimensional space is a multi-objective multi-constraint optimization problem. The objectives, phasing maneuver and deployment time, and the constraints, carrying capability of rocket, are demonstrated together in Figure 9 to characterize the solution space conveniently.

First, the contour map of phasing maneuver in r_p-α two-dimension space is calculated and is put into the algorithm of mass distribution of launch mass mentioned in Sect. 3.4. The boundary between the acceptable regions of LM-3A and LM-3B is marked in Figure 9 with solid blue line. LM-3A is in the bottom right corner. The perihelion radius of working orbit should be larger than 0.75 AU. Most noteworthy point is that the phase angle is less than 30° unless r_p is larger than 0.85 AU in terms of LM-3A. The rest region in the r_p-α plane means that the LM-3B could be the proper candidate for launcher.

Then, the deployment time dt, another crucial index, is calculated and marked with green solid curve in Figure 9. In the acceptable region of LM-3A, fast deployment starts from r_p =0.75 AU and ends at r_p =0.775 AU. However, the maximum value of phase angle α is 20°. The maximum value of phase angle α can reach to 30° by LM-3A when the medium deployment is adopted. In the other words, if we want to deploy the Solar Ring faster and ensure the 30° phase angle α, the rocket of LM-3B should be used as shown the top left corner in Figure 9.

Consequently, three kinds of candidate trajectories are concluded in Figure 9: (1) medium deployment of 0.85 AU r_p and α of 30° launched by LM-3A, (2) fast deployment of 0.7AU r_p and 30 degree α launched by LM-3B, (3) fast deployment with 0.775 AU r_p and α of 20° launched by LM-3A. The trajectory profile with LM-3A will take more time, about 6.5 years, to accomplishment the constellation deployment, or sacrifice phase angle α to 20° to ensure the fast deployment in about 4.4 years. However, trajectory profile with LM-3B, at the cost as expensive as two times of that of LM-3A, can realize the fast deployment within 3.6 years and 30° phase angle simultaneously.

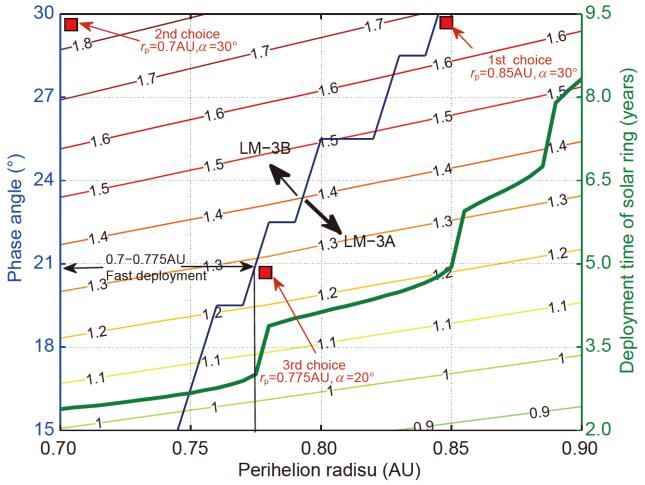

Figure 9 Comprehensive contour map mixed with deployment time, rocket evaluation (the contour lines in this figure is the phasing maneuver with the unit of km/s).

4 Three candidate mission profiles

4.1 Medium deployment with 0.85 AU perihelion and α of 30° by LM-3A

The optimal phasing trajectory to generate 30° phase angle is designed by the method mentioned in Sect. 3.1 and is shown in Figure 10. In order to reduce fuel consumption, the "behind" deployment is adopted. Two spacecraft, A_1 and A_2, are launched into 0.85×1 AU orbit with one rocket at time T_0. After 0.445-year flight together, the phasing spacecraft A_1 executes the first phasing maneuver, ΔV_1=0.84 km/s to insert into the phasing trajectory. The orbital period of phasing orbit is 0.967-year which results in the spacecraft A_1 30° behind spacecraft A_1 after a period. When spacecraft A_1 return to the working orbit, the second phasing maneuver, ΔV_2=0.84 km/s, is executed. The phasing process takes 0.445 +0.967=1.412 years and 0.84 + 0.84 = 1.68 km/s.

The launch window of the second group of the spacecraft appears 2.54 years after the first launch referring to Sect. 3.3. The third group will be launched at the time of T_0+5.08 years. The total time for accomplishment of three-group deploy-

ment is 6.5 years, i.e., 2371.5 days. The magnitude of phasing maneuver and time of phasing trajectory for the second and third group is the same as that of the first group. The Solar Ring of the three groups with 0.85×1 AU orbits is shown in Figure 11.

The launch energy C_3 is 1.52 km^2/s^2 and the upper limit for LM-3A is 1375 kg. Suppose that the dry mass of spacecraft is 460 kg. According to the distribution strategy of mass stated in Sect. 3.4, the mass for spacecraft A_1 is 875 kg with margin of 43 kg and for A_2 is 500 kg with margin of 40 kg, respectively. The total maneuver for spacecraft A_1 is 1.68 km/s which requires 372 kg fuel with 310 s bi-propellant thruster. The fuel margin will be considered in the detailed design of mission in the future. The mass distribution for spacecraft A_1 and A_2 are listed in the Table 1.

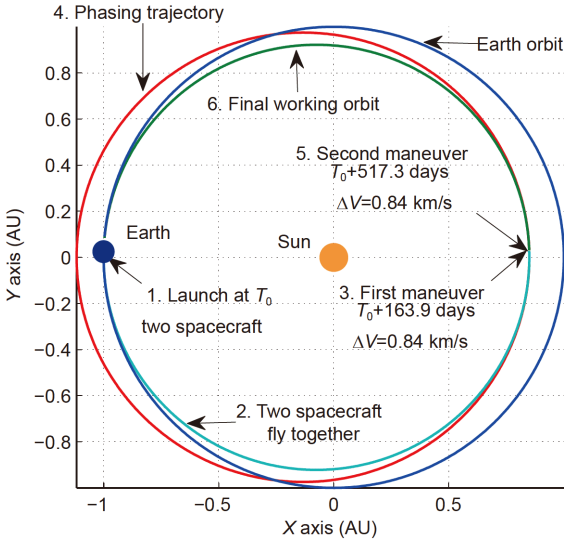

Figure 10 Optimal phasing trajectory of spacecraft.

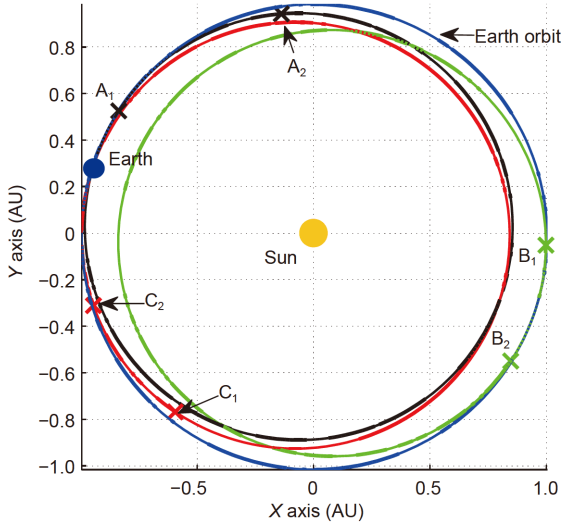

Figure 11 The trajectory of solar ring with 0.85 perihelion and 1AU aphelion.

For the scientists, 30° phase angle α within a group and 120° phase angle β between each group is an optimal observation geometry. However, the angles are time-varying for the 0.85×1 AU elliptical orbit. The simulation result shown in Figure 12 depicts the variation curves of phase angle α and β. The phase angle α is in the vicinity of 30° and ranges between 23° and 37° with the period of 0.882 year. The phase angle β between the 1st and 2nd groups is from 111°–132°, between the 2nd and 3rd groups is from 118°–126°, and between the 3rd and 1st groups is from 103°–127°. It is necessary to take the variation of phase angle α and β into account, when the observation strategy and science payloads are designed.

4.2 Fast deployment with 0.7 AU perihelion and 30° α by LM-3B

Excluding the dry mass of two spacecraft, about 900 kg, there is no sufficient mass for the fuel of phasing maneuver since the carrying capability of LM-3A for 0.7×1 AU orbit is only 1070 kg. In this case, the more demanding rocket, LM-3B would be another option. The optimal phasing trajectory with "behind" deployment is designed. The first phasing maneuver, ΔV_1=0.94 km/s, is executed at time T_0+0.394 year. Then, spacecraft A_1 inserts into a phasing orbit of 0.871-year orbital period. After one-period flight, the phasing spacecraft performs the second maneuver, ΔV_2=0.94 km/s, and return to the 0.7×1 AU working orbit. Then, the phasing spacecraft is

Table 1 Mass distribution of two spacecraft with one rocket of LM-3A

Item	Spacecraft	
	A2 (non-maneuver)	A1 (phasing maneuver)
Dry mass (kg)	460	460
Fuel mass (kg)	0	372
Margin (kg)	40	43
Total mass (kg)	500	875
Thruster and isp	–	bi-propellant, 310 s

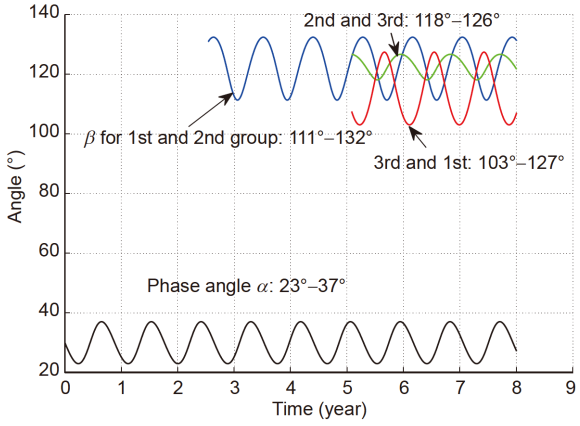

Figure 12 Phase angle α and β vary with time.

30° behind the other spacecraft. The phasing process takes 1.265 years and 1.88 km/s.

The second group of spacecraft will be launched at T_0 +1.19 years. The time of the third group is T_0+2.38 years. The total time for accomplishment of the three-group deployment is 3.65 years, i.e., 1330.3 days. For this working orbit, the launch energy C_3 is 7.60 km^2/s^2 and the launch mass of LM-3B is 2760 kg. According to the strategy stated in Sect. 3.4, the mass for spacecraft A_1 is 950 kg with margin of 51 kg and for A_2 500 kg with margin of 40 kg, respectively. The total maneuver for spacecraft A_1 is 1.88 km/s which requires 439 kg fuel with 310 s bi-propellant thruster. The remaining mass in this launch is 1310 kg which can be used for piggybacking other deep-space missions.

4.3 Fast deployment with 0.775 AU perihelion and α of 20° by LM-3A

According the comprehensive analysis in Sect. 3.5, both fast deployment and low launch cost can be achieved if the phase angle α is smaller than 20°. Even though the optimal observatory geometry in the view of science requires α=30°, the working orbit with 0.775 AU perihelion and α of 20° is still recommended because of the advantages in deployment time and launch cost. The phasing trajectory with "behind" deployment is designed and optimized. The strategy of phasing trajectory is similar to the other two trajectory profiles. The phasing spacecraft A_1 arrives at 20° behind the spacecraft A_2 after two maneuvers with total ΔV=1.24 km/s and flight time of 1.311 year. The time interval for each launch is 1.56 years. The total time for accomplishment of three-group deployment is 4.43 year, i.e., 1617.2 days. As for this working orbit, the launch energy C_3 is 3.81 km^2/s^2 and the launch mass of LM-3A is 1260 kg. The mass for spacecraft A_1 is 760 kg with margin of 45 kg and for A_2 500 kg with margin of 40 kg, respectively. The total maneuver for spacecraft A_1 is 1.24 km/s which requires 255 kg fuel with 310 s bi-propellant thruster.

5 Conclusions

In this paper, the preliminary mission design of the Solar Ring mission has been presented. The phasing maneuver, deployment time of the Solar Ring, and carrying capability of rockets are analyzed comprehensively in the r_p-α space. Three feasible profiles are identified for consideration.

(1) Medium deployment by LM-3A with the working orbit of r_p=0.85 AU and α=30°: the first group of the spacecraft can be deployed in 1.42 years, two groups in 3.96 years, and the whole mission in 6.5 years.

(2) Fast deployment by LM-3B with the working orbit of r_p=0.7 AU and α=30°: the first group of the spacecraft can be deployed in 1.26 years, two groups in 2.45 years, and the whole mission in 3.65 years.

(3) Fast deployment by LM-3A with the working orbit of r_p=0.775 AU and α=20°: the first group of the spacecraft can be deployed in 1.31 years, two groups in 2.87 years, and the whole mission in 4.43 years.

Launch with LM-3A costs more time, about 6.5 years, to accomplish the constellation deployment, otherwise the 4.43 years cost is based on the phase angle α cutting down. However, launch with LM-3B, which is two times more expensive than LM-3A, can realize the fast deployment within 3.65 years and 30° phase angle simultaneously. If considering that some core science objectives of the Solar Ring mission can be immediately achieved after the separation of the two spacecraft in the first group, the medium deployment by LM-3A is affordable as the spacecraft of the first group start to separate after 0.45 years and complete the 30° phase angle in 1.42 years.

This work was supported by the Strategic Priority Program of Chinese Academy of Sciences (CAS) (Grant Nos. XDA15017300 and XDB41000000), and the Youth Innovation Promotion Association CAS (Grant No. 2020295).

1 Kaiser M L, Kucera T A, Davila J M, et al. The stereo mission: An introduction. Space Sci Rev, 2008, 136: 5–16
2 Domingo V, Fleck B, Poland A I. SOHO: The solar and heliospheric observatory. Space Sci Rev, 1995, 72: 81–84
3 Ogilvie K W, Parks G K. First results from WIND spacecraft: An introduction. Geophys Res Lett, 1996, 23: 1179–1181
4 Stone E C, Frandsen A M, Mewaldt R A, et al. The advanced composition explorer. Space Sci Rev, 1998, 86: 1–22
5 Handy B N, Acton L W, Kankelborg C C, et al. The transition region and coronal explorer. Sol Phys, 1999, 187: 229–260
6 Ogawara Y, Takano T, Kato T, et al. The solar-a mission: An overview. Sol Phys, 1991, 136: 1–16
7 Pesnell W D, Thompson B J, Chamberlin P C. The solar dynamics observatory (SDO). Sol Phys, 2012, 275: 3–15
8 Kosugi T, Matsuzaki K, Sakao T, et al. The Hinode (solar-b) mission: An overview. Sol Phys, 2007, 243: 3–17
9 Müller D, Marsden R G, St. Cyr O C, et al. Solar orbiter. Sol Phys, 2013, 285: 25–70
10 Fox N J, Velli M C, Bale S D, et al. The Solar Probe Plus mission: Humanity's first visit to our star. Space Sci Rev, 2016, 204: 7–48
11 Gan W Q, Zhu C, Deng Y Y, et al. Advanced space-based solar observatory (ASO-S): An overview. Res Astron Astrophys, 2019, 19: 156
12 Lyu S Y, Li X L, Wang Y M, et al. Optimal stereoscopic angle for reconstructing solar wind inhomogeneous structures. Adv Space Res, submitted, 2020. arXiv: 2005.06838
13 Wang Y M, Ji H S, Wang Y M, et al. Concept of the Solar Ring Mission: Overview. Sci China Tech Sci, doi: 10.1007/s11431-020-1603-2
14 China Great Wall Industry Corporation. LM-3A Series Launch Vehicles User's Manual. Beijng, 2011
15 Guibout V M, Scheeres D J. 3-Solving two-point boundary value problems using generating functions: theory and applications to astrodynamics. Elsevier Astrodynamics Series, 2006, 1: 53–105
16 Curtis H. Orbital Mechanics for Engineering Students. 3rd Ed. Burlington: Elsevier Butterworth-Heinemann, 2014. 107–145
17 Wuerl A, Crain T, Braden E. Genetic algorithm and calculus of variations-based trajectory optimization technique. J Spacecraft Rockets, 2003, 40: 882–888